Acta Mechanica 99, 35–48 (1993)

ACTA MECHANICA

Natural vibration of cracked rotating beams

M. Krawczuk, Gdańsk, Poland

(Received April 14, 1992)

Summary. The paper presents a finite element model of a rotating cracked beam. A crack occurring in the rotating beam is open. The method of calculation of the characteristics matrices of the cracked beam finite element are presented. The effects of crack location and its depth on the dynamic behavior of the rotating beam are studied. It is found that the crack can change the natural frequencies of the system.

1 Introduction

The crack in structural elements causes a local change of a structure stiffness. Since this stiffness alters inside the considered element its dynamic characteristics, i.e. natural frequencies, amplitudes of forced vibrations, the regions of stability alter as well. The dynamic behaviour of cracked structures depends upon crack location, depth, shape as well as upon analyzed form of vibration.

Bibliography given by Wauer [1] concerning the influence of cracks on dynamic behaviour of different structures is extensive. However, only a few papers are devoted to analysis of the rotating blades and beams. Modelling and formulation of the equations of motion for the cracked rotating blade were studied by Wauer [2]. He states that the resulting equations of motion for small superimposed vibrations are completely linear. Chen and Chen [3] presented the model of the cracked blade which may be restricted to very low angular speeds. The reduction impact of the crack on natural frequencies and areas of stability were reported by them. Chen and Shen [4] presented the model of the rotating cracked blade made of an orthotropic material. The influence of the crack location, its depth and angle between the composite fibre and the blade longitudinal axis on the natural frequencies were analyzed.

The main objective of this paper is to elaborate the beam finite element with one-edge open crack and to analyze the influence of this crack on the natural frequencies of the rotating beam. Because the rotating beam is tensed a non-breathing model of the crack is assumed. The displacement finite element method is applied, and two different shape functions, for left and right part of the cracked beam element, are defined. The characteristic matrices of the cracked beam finite element are computed i.e. the consistent mass matrix, stiffness matrix, geometrical stiffness matrix and stiffness matrix depending on squared angular velocity. The influence of the crack location and its depth on changes of the natural frequencies are illustrated with two numerical examples.

2 A finite element model

The beam element of a rectangular cross-section with one-edge crack is presented in Fig. 1. A general loading is indicated by the four general forces $P_1, \ldots, P_4$ at a node. The element of length l has the crack at distance l_1 from its left end, where $0 < l_1 < l$. In a general case the crack introduces a discontinuity at l_1, in both the deflection and slope, due to the bending and shear compliance. In the presented model only discontinuity in slope due to the bending is introduced. Therefore, at Sections 1 and 2, two different shape functions will be defined as the third order polynomials

$$\begin{aligned} u_{11} &= a_1 + a_2 x + a_3 x^2 + a_4 x^3, \\ u_{12} &= a_5 + a_6 x + a_7 x^2 + a_8 x^3, \end{aligned} \tag{1}$$

$$\begin{aligned} u_{21} &= a_9 + a_{10} x + a_{11} x^2 + a_{12} x^3, \\ u_{22} &= a_{13} + a_{14} x + a_{15} x^2 + a_{16} x^3. \end{aligned} \tag{2}$$

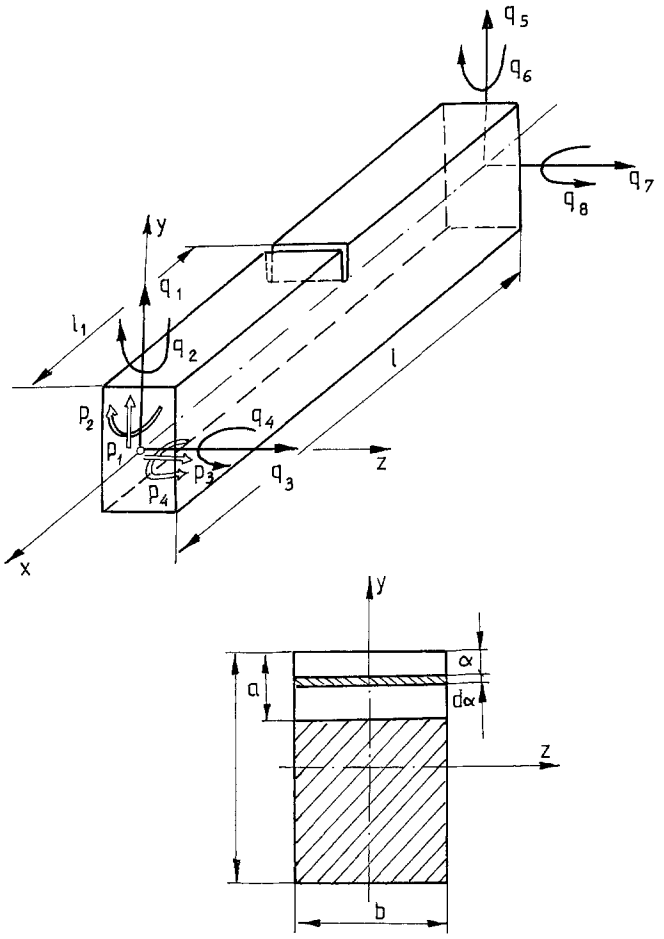

Fig. 1. A beam finite element with one-edge open crack

Application of the following boundary conditions at the beam ends:

$$\begin{aligned} q_1 &= u_{11}|_{x=0} \quad & q_5 &= u_{12}|_{x=l}, \\ q_2 &= u'_{11}|_{x=0} \quad & q_6 &= u'_{12}|_{x=l}, \\ q_3 &= u_{21}|_{x=0} \quad & q_7 &= u_{22}|_{x=l}, \\ q_4 &= u'_{21}|_{x=0} \quad & q_8 &= u'_{22}|_{x=l}, \end{aligned} \tag{3}$$

and continuity and compatibility with bending compliance c_1, c_2 at the crack location

$$\begin{aligned} &u_{11}(l_1) = u_{12}(l_1) \\ &u'_{12}(l_1) = u'_{11}(l_1) + c_1 u''_{11}(l_1) \\ &u''_{11}(l_1) = u''_{12}(l_1) \\ &u'''_{11}(l_1) = u'''_{12}(l_1) \\ &u_{21}(l_1) = u_{22}(l_1) \\ &u'_{22}(l_1) = u'_{21}(l_1) + c_2 u''_{21}(l_1) \\ &u''_{21}(l_1) = u''_{22}(l_1) \\ &u'''_{21}(l_1) = u'''_{22}(l_1) \end{aligned} \tag{4}$$

yield the shape functions

$$\mathbb{N}_1 = \left[\begin{array}{c|c} 1, x, x^2, x^3 & \mathbb{O} \\ \hline \mathbb{O} & 1, x, x^2, x^3 \end{array}\right] \mathbb{G}_1, \tag{5}$$

$$\mathbb{N}_2 = \left[\begin{array}{c|c} 1, x, x^2, x^3 & \mathbb{O} \\ \hline \mathbb{O} & 1, x, x^2, x^3 \end{array}\right] \mathbb{G}_2. \tag{6}$$

The matrices $\mathbb{G}_1$ and $\mathbb{G}_2$, for $l_1 = l/2$, have the forms

$$\mathbb{G}_1 = \begin{bmatrix} 1 & 0 & 0 & 0 & 0 & 0 & 0 & 0 \\ 0 & 1 & 0 & 0 & 0 & 0 & 0 & 0 \\ G_1 & G_2 & 0 & 0 & -G_1 & G_3 & 0 & 0 \\ G_4 & G_5 & 0 & 0 & -G_4 & G_5 & 0 & 0 \\ 0 & 0 & 1 & 0 & 0 & 0 & 0 & 0 \\ 0 & 0 & 0 & 1 & 0 & 0 & 0 & 0 \\ 0 & 0 & G_1 & G_6 & 0 & 0 & -G_1 & G_7 \\ 0 & 0 & G_4 & G_5 & 0 & 0 & -G_4 & G_5 \end{bmatrix}, \tag{7}$$

$$\mathbb{G}_2 = \begin{bmatrix} 1 & G_8 & 0 & 0 & 0 & G_8 & 0 & 0 \\ 0 & G_9 & 0 & 0 & 0 & G_{10} & 0 & 0 \\ G_1 & G_2 & 0 & 0 & -G_1 & G_3 & 0 & 0 \\ G_4 & G_5 & 0 & 0 & -G_4 & G_5 & 0 & 0 \\ 0 & 0 & 1 & G_{11} & 0 & 0 & 0 & G_{11} \\ 0 & 0 & 0 & G_{12} & 0 & 0 & 0 & G_{13} \\ 0 & 0 & G_1 & G_6 & 0 & 0 & -G_1 & G_7 \\ 0 & 0 & G_4 & G_5 & 0 & 0 & -G_4 & G_5 \end{bmatrix}, \tag{8}$$

where

$$
\begin{aligned}
G_1 &= -3/l^2 \\
G_2 &= -3/l^2 - 1/(2l + 2c_1) \\
G_3 &= -3/l^2 + 1/(2l + 2c_1) \\
G_4 &= 2/l^3 \\
G_5 &= 1/l^2 \\
G_6 &= -3/l^2 - 1/(2l + 2c_2) \\
G_7 &= -3/l^2 + 1/(2l + 2c_2) \\
G_8 &= l/2 - l^2/(2l + 2c_1) \\
G_9 &= l/(l + c_1) \\
G_{10} &= c_1/(l + c_1) \\
G_{11} &= l/2 - l^2/(2l + 2c_2) \\
G_{12} &= l/(l + c_2) \\
G_{13} &= c_2/(l + c_2).
\end{aligned} \tag{9}
$$

The non-dimensional flexibilities due to the crack are equal [5]

$$
\begin{aligned}
c_1 &= \frac{12\Pi(1 - \nu^2)\, h}{l} \int_0^{\bar{a}} \bar{\alpha} F_1^{\,2}(\bar{\alpha})\, d\bar{\alpha} \int_0^{1/2} d\bar{z}, \\
c_2 &= \frac{48\Pi(1 - \nu^2)\, h}{l} \int_0^{\bar{a}} \bar{\alpha} F_2^{\,2}(\bar{\alpha})\, d\bar{\alpha} \int_0^{1/2} \bar{z}^2 d\bar{z},
\end{aligned} \tag{10}
$$

where $\bar{\alpha} = \alpha/h$, $\bar{z} = z/b$ (see Fig. 1).

The functions $F_1(\bar{\alpha})$ and $F_2(\bar{\alpha})$, taking into consideration the finite dimensions of the element, have the forms [5]

$$
F_1(\bar{\alpha}) = \sqrt{\tan \lambda/\lambda}\,[0.752 + 2.02\bar{\alpha} + 0.37(1 - \sin \lambda)^3]/\cos \lambda, \tag{11}
$$

$$
F_2(\bar{\alpha}) = \sqrt{\tan \lambda/\lambda}\,[0.923 + 0.199(1 - \sin \lambda)^4]/\cos \lambda, \tag{12}
$$

where $\lambda = \Pi\alpha/2h$.

The changes of the non-dimensional flexibilities as a function of the non-dimensional depth of the crack and slenderness ratio of the beam element h/l are given in Fig. 2.

The matrices of stress-strain relations in this case have the forms

$$
\mathbb{B}_1 = \left[\begin{array}{c|c} 0,\ 1,\ 2x,\ 3x^2 & \mathbb{O} \\ \hline \mathbb{O} & 0,\ 1,\ 2x,\ 3x^2 \end{array}\right] \mathbb{G}_1, \tag{13}
$$

$$
\mathbb{B}_2 = \left[\begin{array}{c|c} 0,\ 1,\ 2x,\ 3x^2 & \mathbb{O} \\ \hline \mathbb{O} & 0,\ 1,\ 2x,\ 3x^2 \end{array}\right] \mathbb{G}_2. \tag{14}
$$

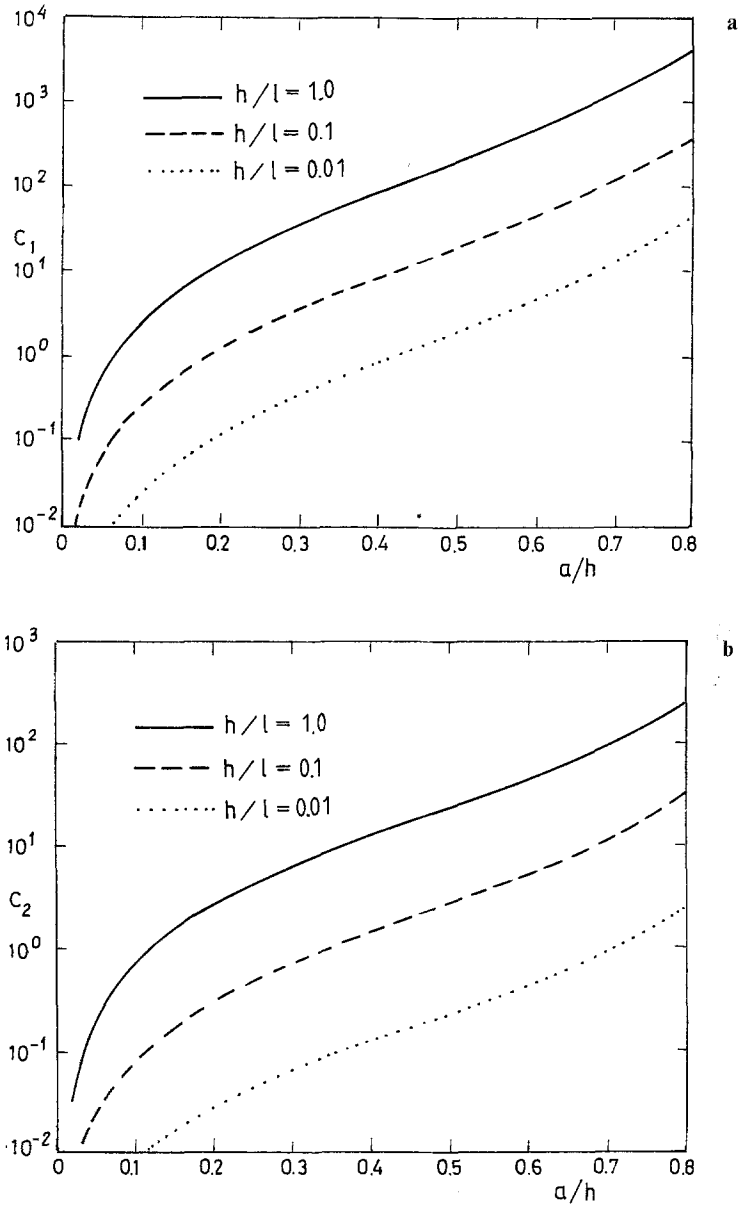

Fig. 2. Non-dimensional coefficients of the flexibility due to the crack; **a** bending compliance c_1 in y-direction **b** bending compliance c_2 in z-direction

The element stiffness matrix is equal

$$\mathbb{K}_e = \int_0^{l/2} \mathbb{B}_1{}^t\mathbb{D}\mathbb{B}_1\, dx + \int_{l/2}^{l} \mathbb{B}_2{}^t\mathbb{D}\mathbb{B}_2\, dx, \tag{15}$$

where $\mathbb{D}$ is the stress-strain relation matrix [6], t is the symbol of transpose of a matrix.

Similarly the geometrical stiffness matrix can be expressed as

$$\mathbb{K}_{ge} = \int_0^{l/2} p_{11}\mathbb{G}_1{}^t\mathbb{F}\mathbb{G}_1\, dx + \int_{l/2}^{l} p_{11}\mathbb{G}_2{}^t\mathbb{F}\mathbb{G}_2\, dx, \tag{16}$$

where p_{11} is an axial force loading the element, and the matrix $\mathbb{F}$ has the form

$$\mathbb{F} = \left[\begin{array}{cccc|cccc} 0 & 0 & 0 & 0 & & & & \\ 0 & 1 & 2x & 3x^2 & & & & \\ 0 & 2x & 4x^2 & 6x^3 & & \Phi & & \\ 0 & 3x^2 & 6x^3 & 9x^4 & & & & \\ \hline & & & & 0 & 0 & 0 & 0 \\ & \Phi & & & 0 & 1 & 2x & 3x^2 \\ & & & & 0 & 2x & 4x^2 & 6x^3 \\ & & & & 0 & 3x^2 & 6x^3 & 9x^4 \end{array}\right]. \tag{17}$$

The matrix of stiffness depending on squared angular velocity can be written as

$$\mathbb{K}_{ce} = \varrho\omega^2 A \int_0^{l/2} \mathbb{N}_1{}^t \mathbb{W}^t \mathbb{W} \mathbb{N}_1 \, dx + \varrho\omega^2 A \int_{l/2}^{l} \mathbb{N}_2{}^t \mathbb{W}^t \mathbb{W} \mathbb{N}_2 \, dx, \tag{18}$$

where $\mathbb{W}$ is the cosine directions matrix [7], ϱ is the mass density and A is the area of cross-section of the element.

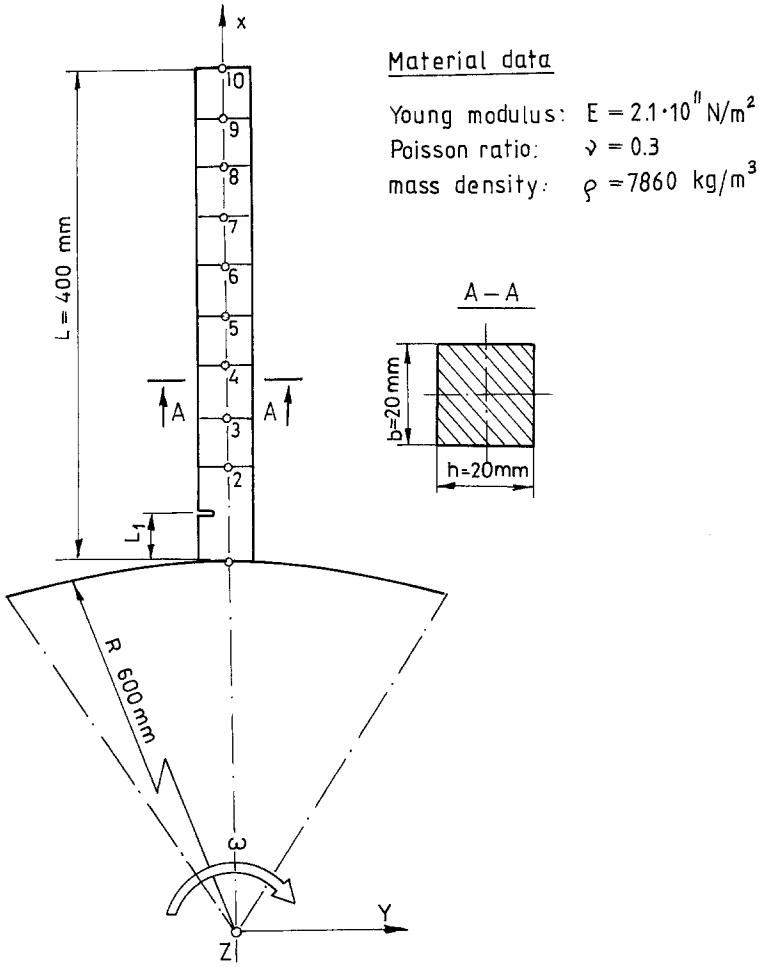

Fig. 3. A rotating cracked beam

The consistent mass matrix for the element is equal

$$\mathbb{M}_e = \varrho A \int_0^{l/2} \mathbb{N}_1{}^t\mathbb{N}_1 \, dx + \varrho A \int_{l/2}^{l} \mathbb{N}_2{}^t\mathbb{N}_2 \, dx. \tag{19}$$

In the case when $c_1 = c_2 = 0$ the forms of the matrices given above are identical to a non-cracked beam finite element of Bernoulli-Euler type [6].

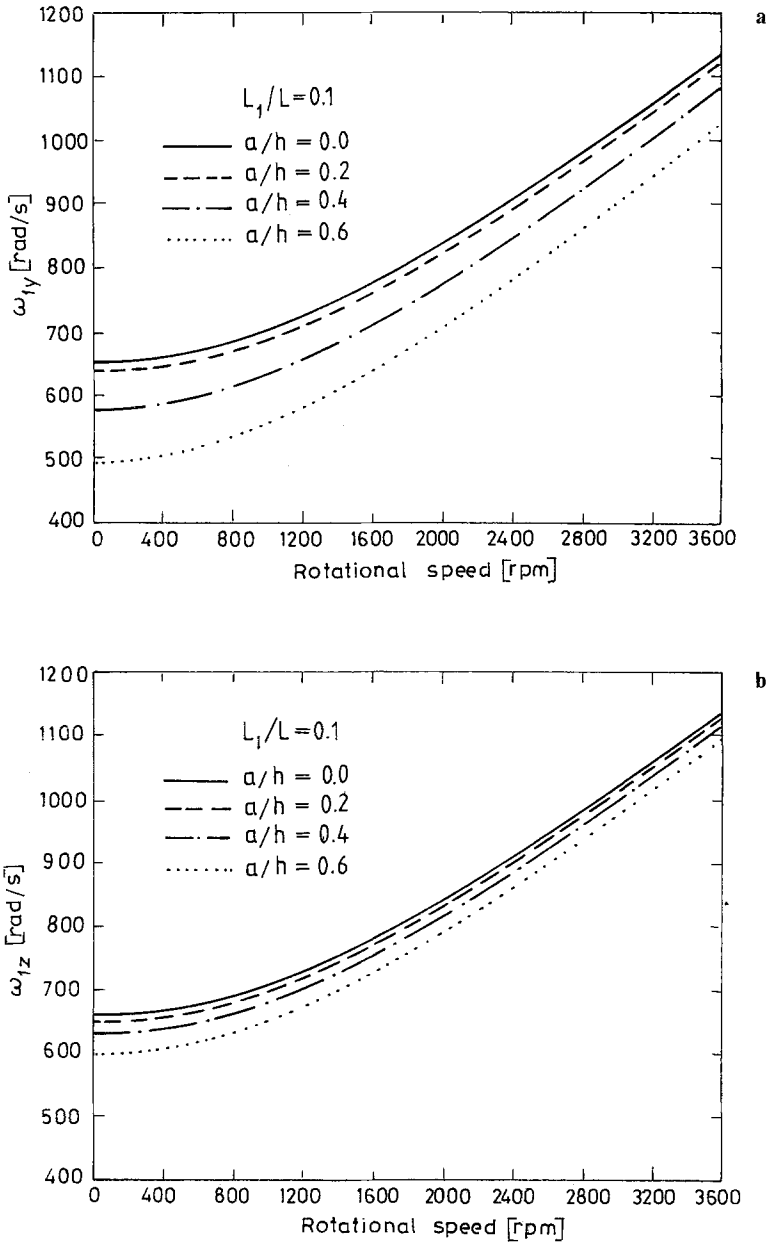

Fig. 4. The change of the first natural frequency as a function of the crack depth; **a** vibration in y-direction **b** vibration in z-direction

3 Vibration of the cracked rotating beam

The cracked beam element developed above was used to study the dynamic behaviour of a cracked rotating beam, the geometrical and material data of which are given in Fig. 3.

The mathematical model of the natural vibration of rotating linear body discretized by finite elements was set up in the form [7]

$$\mathbb{M}\ddot{q} + (\mathbb{K} + \mathbb{K}_g + \mathbb{K}_c)\,\bar{q} = \Phi, \tag{20}$$

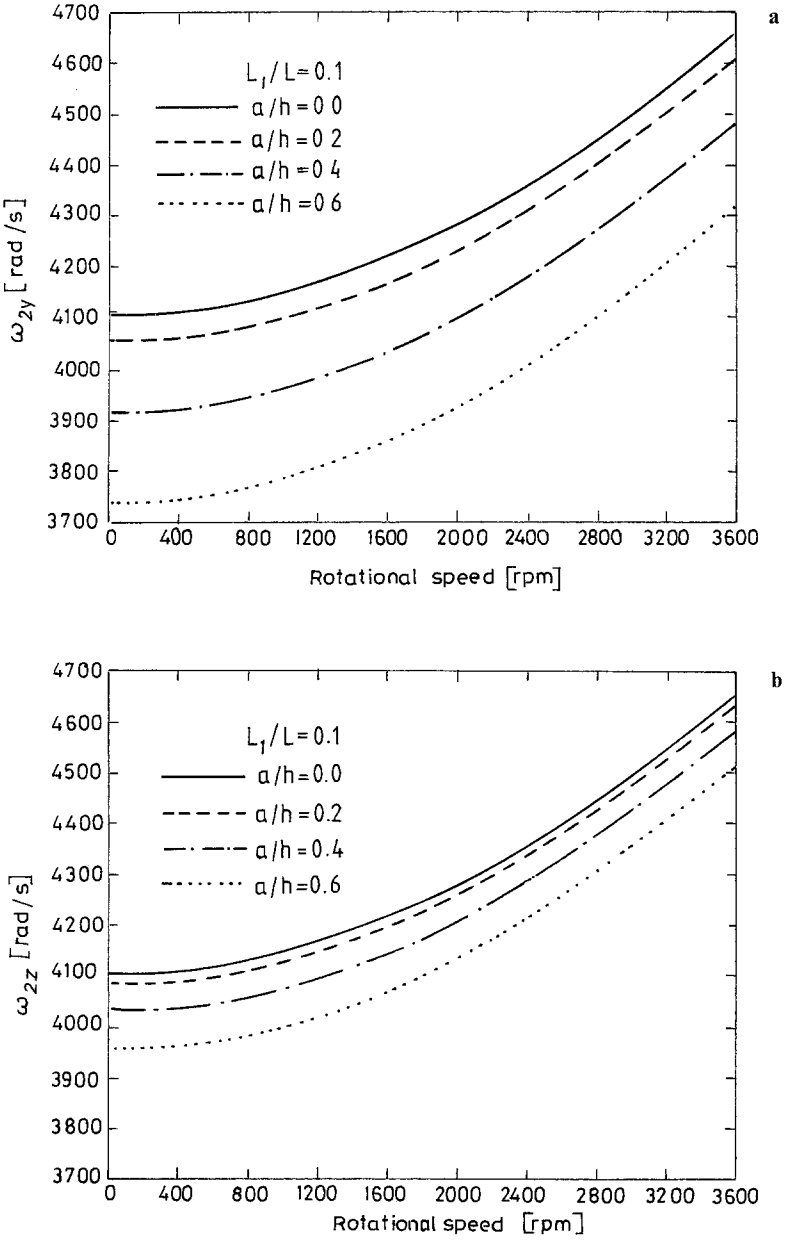

Fig. 5. The change of the second natural frequency as a function of the crack depth; **a** vibration in y-direction **b** vibration in z-direction

where $\mathbb{M}$ is the global matrix of inertia, $\mathbb{K}$ is the global matrix of linear stiffness, $\mathbb{K}_g$ is the global matrix of geometrical stiffness, $\mathbb{K}_c$ is the global matrix of stiffness matrix depending on squared angular velocity, and $\ddot{\bar{q}}$, $\bar{q}$ are the column matrices of generalized accelerations and displacements, respectively.

Figures 4–6 show changes of three natural frequencies of the rotating beam with one crack located at the distance equal 40 mm from the fixed end. The changes of the natural frequencies are plotted for $a/h = 0$, 0.2, 0.4, 0.6 and rotational velocities from 0 to 3600 rpm. Progressive reduction in the resonant frequencies depending on the crack depth is observed.

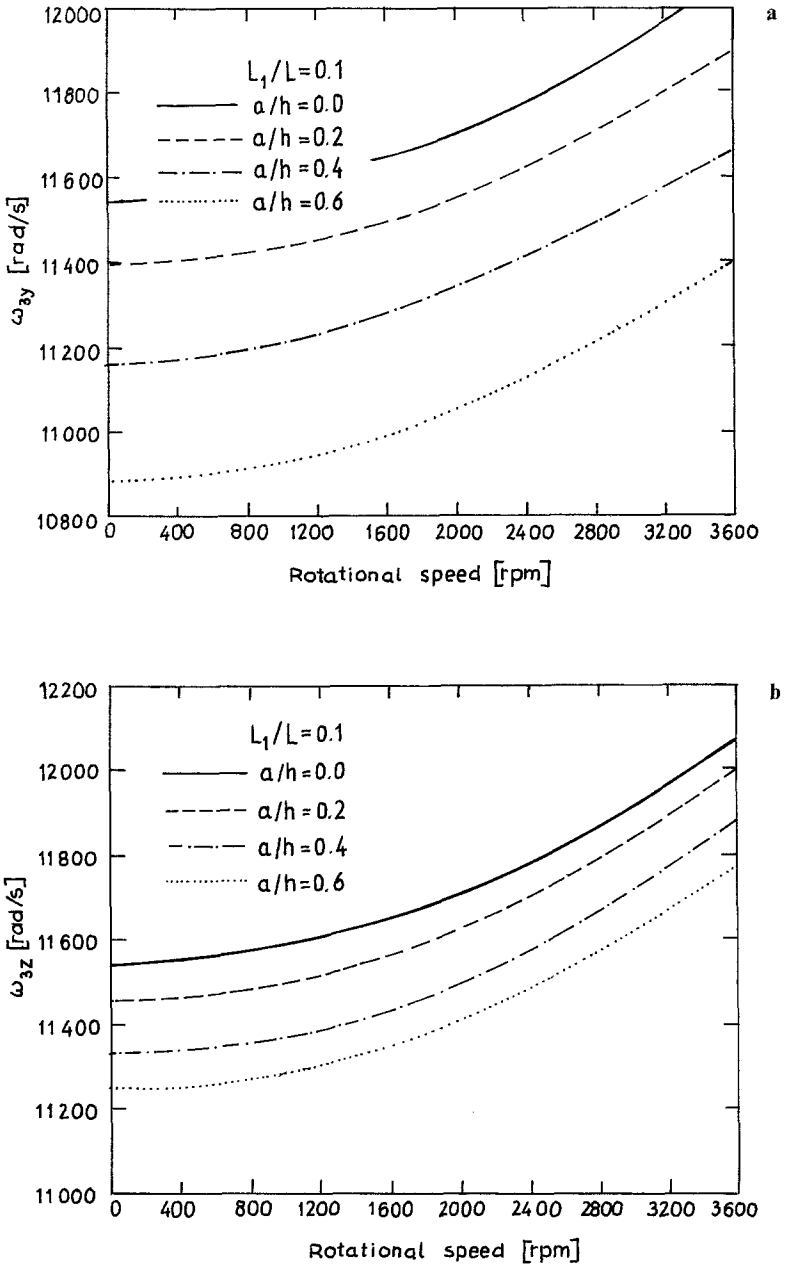

Fig. 6. The change of the third natural frequency as a function of the crack depth; **a** vibration in y-direction **b** vibration in z-direction

The changes of three natural frequencies of the rotating beam with one crack with depth equal 8 mm are presented in Figs. 7–9. The changes of the resonant frequencies are plotted for $L_1/L = 0.1, 0.3, 0.5, 0.7$ and rotational velocities from 0 to 3600 rpm. It is clearly shown that the reduction in the resonant frequencies depends on the mode of vibration.

Figure 10 presents the changes of the bending natural frequencies in two perpendicular directions of vibrations. We can easily notice that these changes are different for each direction.

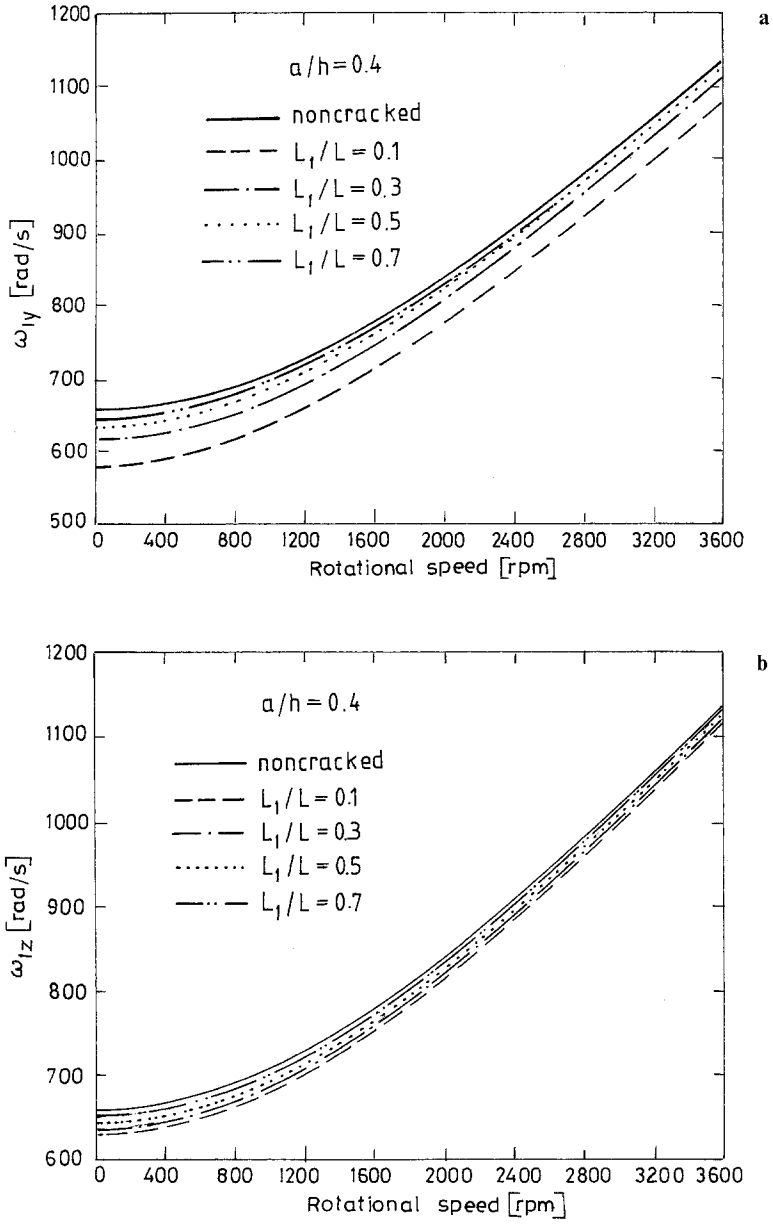

Fig. 7. The change of the first natural frequency as a function of the crack location; **a** vibration in y-direction **b** vibration in z-direction

4 Conclusions

The method of generation of the characteristic matrices of the beam finite element with the one-edge open crack is presented in the paper. The method of creation of the shape functions discussed in the work enables the construction of the beam finite elements with cracks of different types (double-edge, skew, internal, elliptical, etc.) if only the local flexibility for a given type of the crack is known.

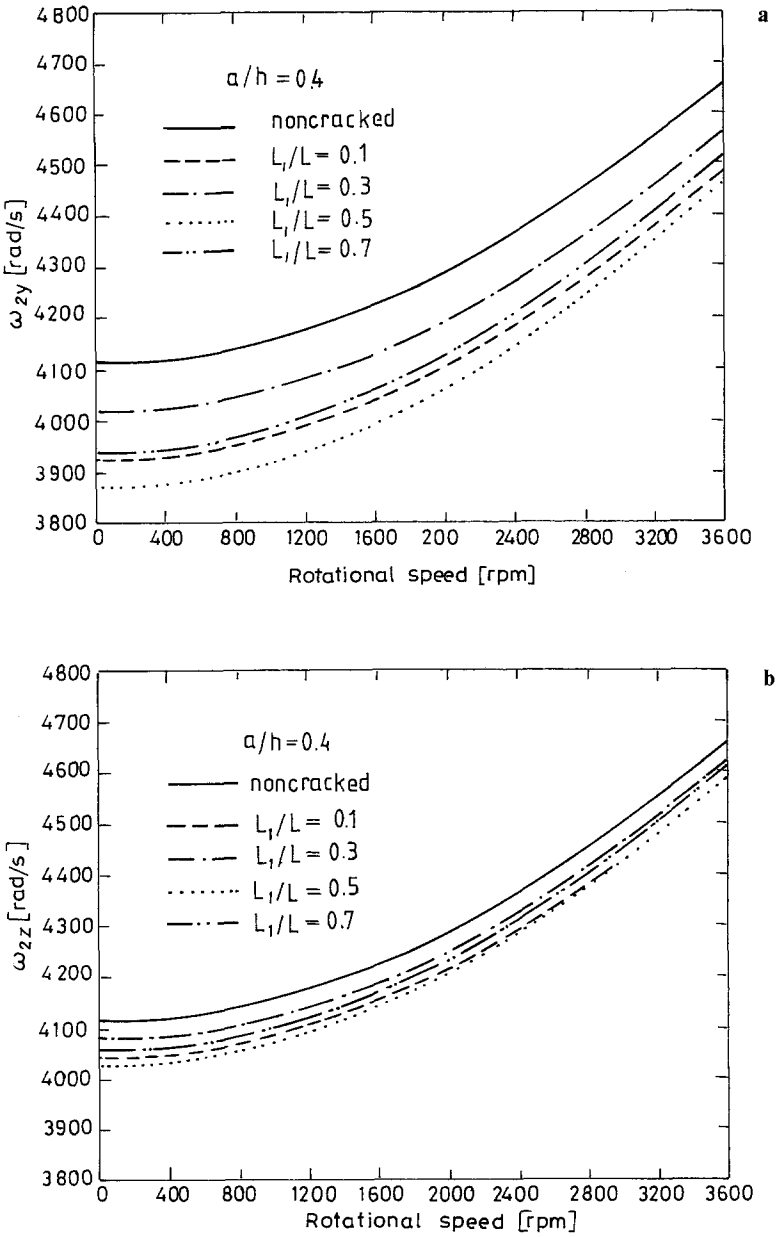

Fig. 8. The change of the second natural frequency as a function of the crack location; **a** vibration in y-direction **b** vibration in z-direction

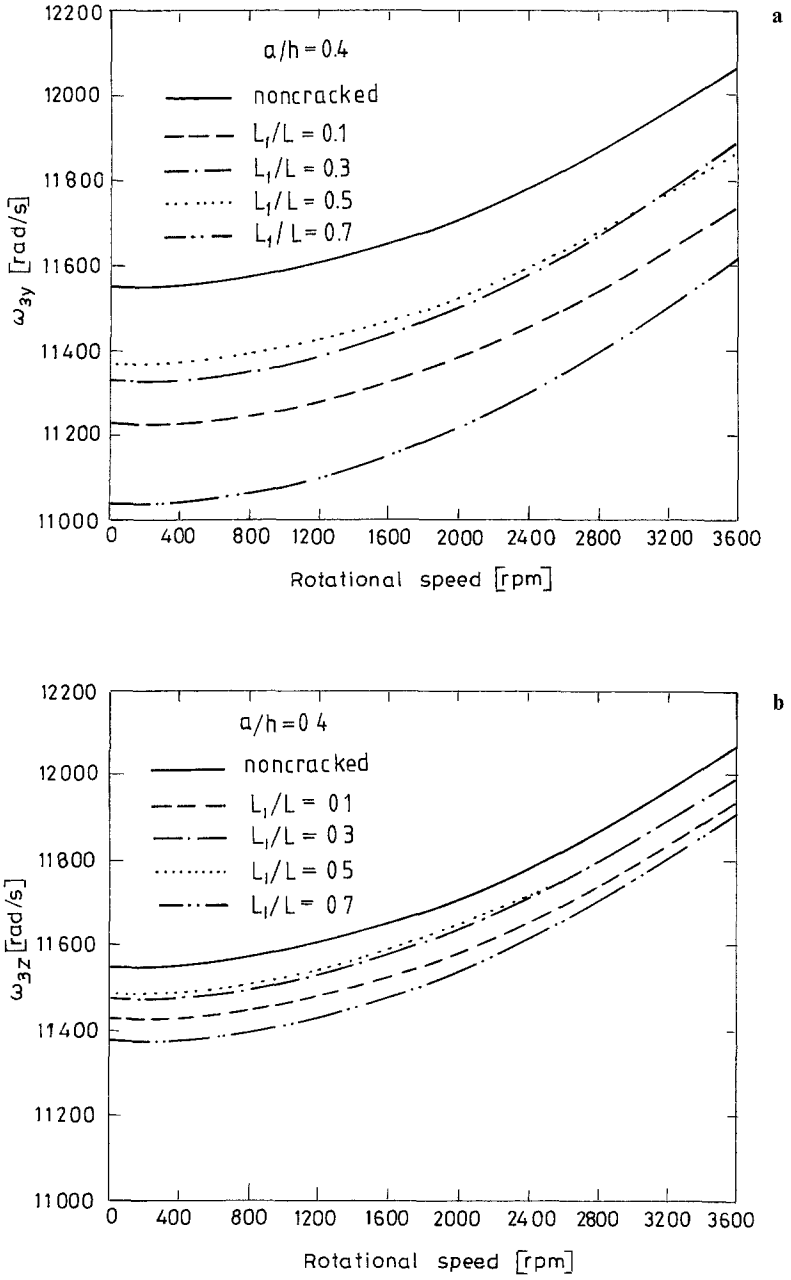

Fig. 9. The change of the third natural frequency as a function of the crack location; **a** vibration in y-direction **b** vibration in z-direction

The results of the numerical calculations have confirmed that the changes of the natural frequencies of the rotating beam are a function of the depth and position of the crack. When the depth of the crack increases, the reducing effect of the crack in natural frequencies also increases. The influence of the crack position on the change of the natural frequencies is connected with the vibration mode. The change of the natural frequencies corresponding to the mode vibration is biggest when the crack is located at the points for which an amplitude of the mode of vibration is equal to zero. On the other hand, when the crack is located at points for

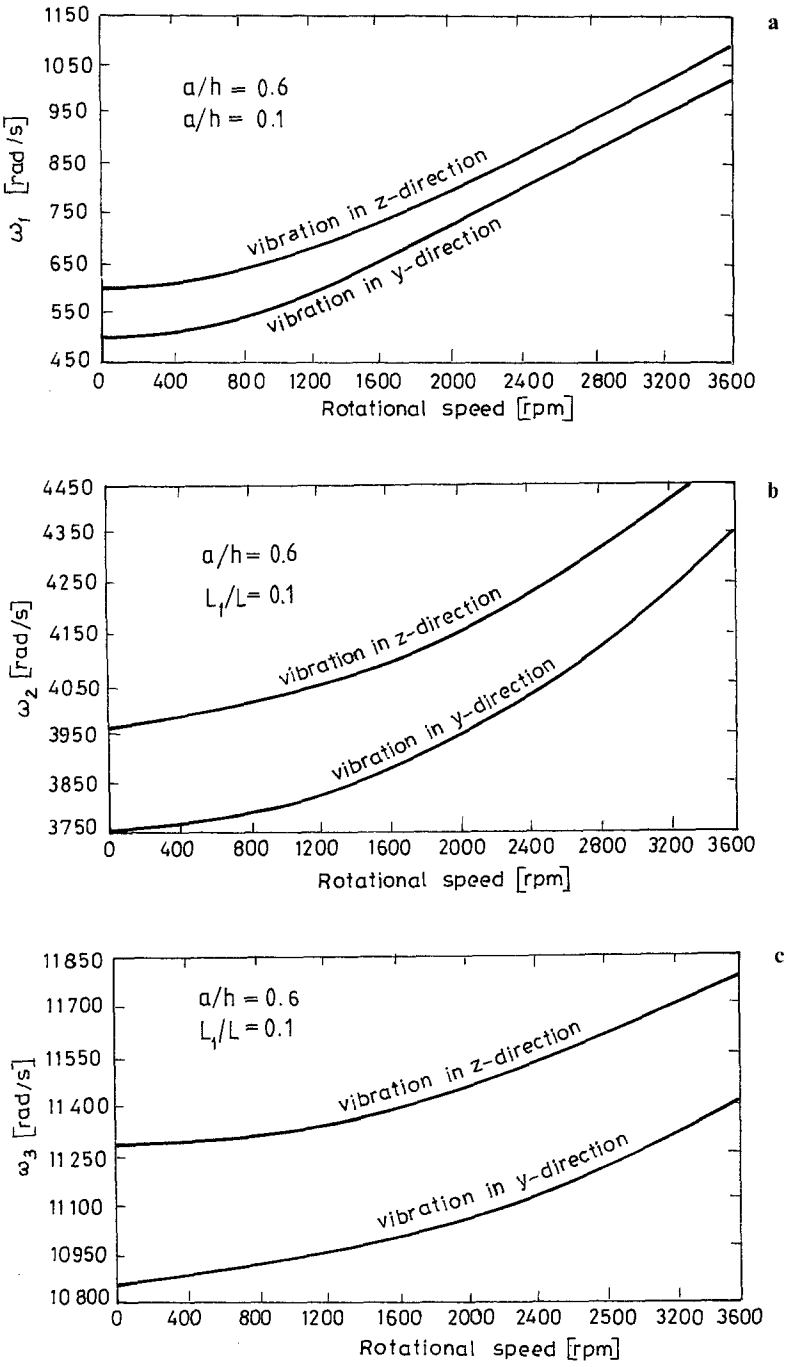

Fig. 10. The change of the bending natural frequency in two perpendicular directions; **a** first mode **b** second mode **c** third mode of vibrations

which an amplitude of the mode of vibration is maximal, the change of the natural vibration is negligible.

The changes of the bending natural frequencies in two perpendicular directions are different. This effect can be used for the crack identification. This problem will be considered in future reports.

References

[1] Wauer, J.: On the dynamics of cracked rotors: a literature survey. Appl. Mech. Rev. **43**, 13–17 (1991).
[2] Wauer, J.: Dynamics of cracked rotating blades. Appl. Mech. Rev. **44**, 273–278 (1991).
[3] Chen, L.-W., Chen, C.-L.: Vibration and stability of cracked thick rotating blades. Comput. Struct. **28**, 67–74 (1988).
[4] Chen, L.-W., Shen, G.-S.: Vibration analysis of a rotating orthotropic blade with an open crack by the finite element method. Proceedings of 3rd International Conference on Rotordynamics, pp. 155–160. Lyon, France 1990.
[5] Papadopoulos, C. A., Dimarogonas, A. D.: Coupled longitudinal and bending vibrations of a cracked shaft. Transactions of the ASME, Journal of Vibration, Acoustic, Stress and Reliability in Design **110**, 1–8 (1988).
[6] Desai, Ch., Abel, J.: Introduction to the finite element methods. New York: Van Nostrand Reinhold 1972.
[7] Bossak, M., Zienkiewicz, O. C.: The vibration of initially stressed solids, with particular referenc to centrifugal-force effects in rotation machinery. J. Strain Anal. **8**, 245–252 (1973).

Author's address: Dr. inż. M. Krawczuk, Polish Academy of Sciences, Institute of Fluid Flow Machinery, ul. Gen. J. Fiszera 14, 80-952 Gdańsk, Poland